

## Simulations of the Gulf of Maine Storm Response Subject to Surface Wave-Induced Effects on Bottom Friction

Y. Fan and W. S. Brown

Ocean Process Analysis Laboratory  
Institute for the Study of Earth Oceans and Space  
Department of Earth Sciences  
University of New Hampshire  
Durham, NH 03824

C. Naimie

Thayer School of Engineering  
Dartmouth College  
Hanover, NH

### Abstract

The 3-D QUODDY barotropic model tests were run for the period of February 7 - 18, 1987 with both a time-space constant drag coefficient  $C_d$  and a time-space variable  $C_d$ . The constant  $C_d$  QUODDY test captured more than 60% of the observed variance, as compared to the 31% of the variance captured by the linear harmonic finite element model FUNDY. Thus the use of a constant  $C_d$  thus represents an improvement in coastal modeling effects. However, there still were large differences between model results and observations in or around the times of intense storms (e.g. February 9<sup>th</sup> to 13<sup>th</sup>). The QUODDY tests with a variety of realistic  $C_d$  values did not improve model results significantly. Neither did the use of time and space variable  $C_d$ . The model behavior was most sensitive to the specification of surface wind stress forcing. Thus, we expect that model improvements may come with a better understanding of the wind stress calculation in the Gulf, perhaps a more detailed understanding of the waves in the whole Gulf of Maine, and the inclusion of atmospheric pressure of the model.

### 1. Background

The Gulf of Maine is an inland sea is separated from the Atlantic Ocean by several shallow offshore banks including Georges Bank ([Figure 1](#)). Thus the Gulf responds to wind fluctuations more like an enclosed basin than an open shelf ([Brown, 1998](#)). The Gulf's complex bathymetry, which includes three deep basins – Georges, Jordan and Wilkinson - further complicates the sea level response to storms in the region.

While occasional hurricanes pass through the region during summer, Gulf region winds are generally much stronger during due to the greater frequency of relatively strong storms that time of year. During the winter stormy season, the Gulf barotropic pressure (i.e. sea level) field responds most strongly to near

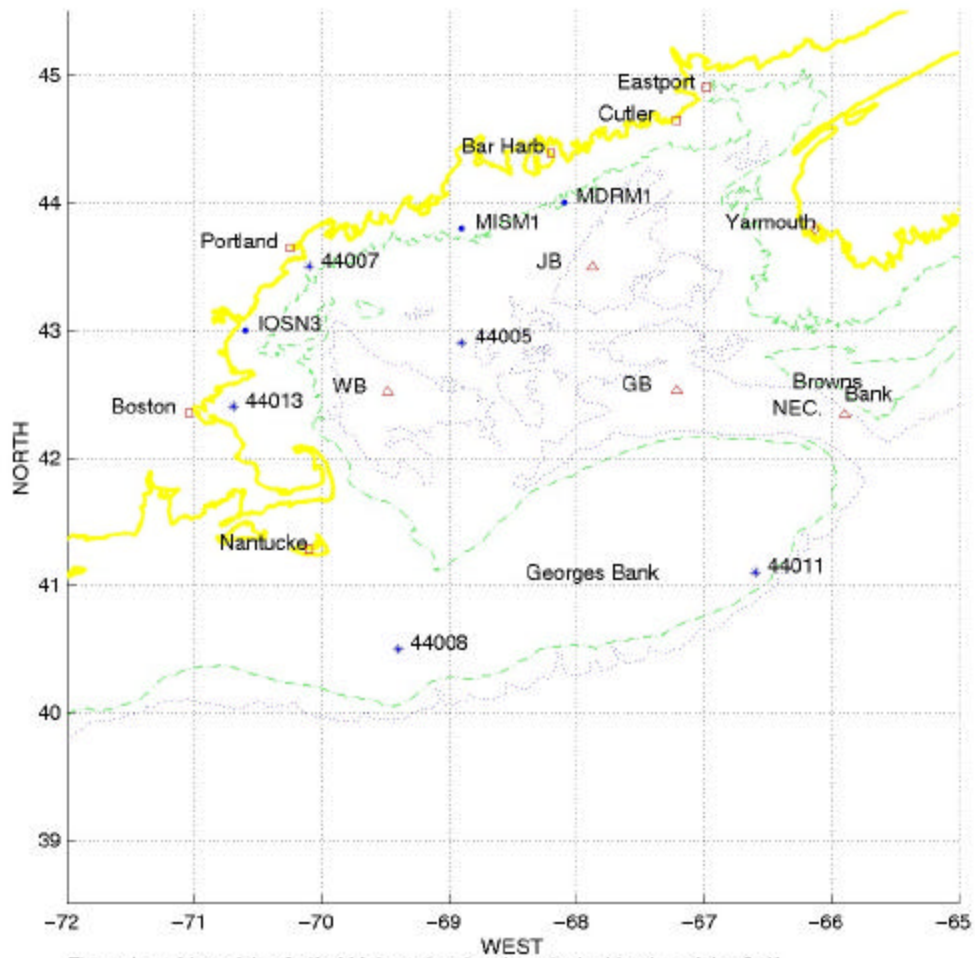


Figure I.1.1 Map of the Gulf of Maine, showing the principal basins of the Gulf and the major shore banks. The NDBC ( ) and C-Man ( ) meteorological stations, and Canadian Marine Environmental Data Service sea level stations ( [ ] ); National Ocean Service sea level stations ( [ ] ); and Bottom Pressure Stations ( ) are shown in the map. The dash-dot line: -.-. refers to the 100m isobath, and the dotted line: ..... refers to the 200m isobath.

Figure 1 (I.1.1)

west-east (255°T-75°T) wind stress fluctuations concentrated in the so-called 2- to 10-day "weather band". A typical Gulf-scale westward wind stress of about 1 Pascal forces general increases in the Gulf-scale sea level pressure of about 10 millibars (mbar~ equivalent centimeter). The related increases in the western Gulf are about 50% higher.

During storms the amplitude of the meteorologically-forced sea levels can be more than a meter more than normal. The weather-band sea level variability is superposed on the primarily semidiurnal tidal variability of the Gulf. In addition, surface waves variability generated by both distant and local winds adds to the sea level variability due to these other causes.

In this paper, we explore the natural storm response of the Gulf sea level. Our approach is to employ a coupled 3-D circulation and bottom boundary layer model (forced by wind and surface waves) to simulate the winter storm response of the Gulf. We used the barotropic version of a three-dimensional, finite-element circulation model named QUODDY (Lynch et al., 1996; 1997) with a time-space constant bottom drag coefficient, to simulate the Gulf of Maine response to realistic winds between 4 and 18 February 1987. We then coupled the Styles and Glenn (2000) bottom boundary layer model (BBLM) to QUODDY and forced it with the same winds. We compare the model-produced sea level results with the pressure observations.

## 2. The Observations

We chose 4-18 February 1987 study period, because there was a comprehensive set of observations that spanned the strong 9-10 February storm. The hourly wind vectors (Figure 2) were obtained from several National Data Buoy Center (NDBC) buoys and National Weather Service (NWS) C-Man island stations throughout the Gulf (see Figure 1 for locations). Hourly winds were optimally- estimated for every node of the Gulf of Maine QUODDY mesh as seen in the Figure 3 example for 21:00 February 9, 1987.

The wind stresses needed to force QUODDY were computed from the optimally-interpolated winds according to the method of Large and Pond (1981). That is the buoy wind speeds were adjusted to a 10m reference height ( $U$ ) and the wind stress was calculated according to

$$\mathbf{t} = \mathbf{r}_{air} C_w U |U| \quad , \quad (1)$$

where if  $|U| < 11\text{m/s}$ , then  $C_w = 1.2 \times 10^{-3}$ ; if  $11\text{m/s} < |U| < 25\text{m/s}$  then  $C_w = (0.49 + 0.065|U|) \times 10^{-3}$ . The density of air is assumed to be  $1.22\text{kgm}^{-3}$ .

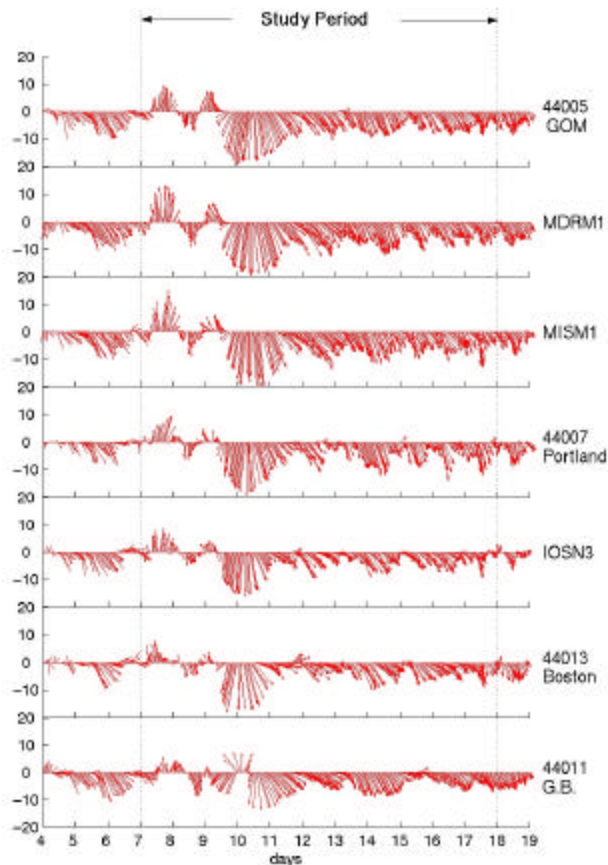


Figure V.2.1 Hourly wind vectors at stations located in Figure I.1.1. The model simulation period is highlighted on the plot.

**Figure 2 (V.2.1)** Hourly wind vectors at a suite of NDBC buoy and NWS C-Man stations in the Gulf of Maine. See Figure 1 for locations.

The wave information used to force the BBLM was obtained at the 5 NDBC stations in the Gulf of Maine (see [Figure 1](#) for locations). This wave information consists of significant wave height ([Figure 4](#)), dominant wave period ([Figure 5](#)), average wave period, and mean wave direction.

Hourly coastal sea level records were obtained from NOAA National Ocean Service (NOS) and Canadian Marine Environmental Data Service (MEDS) for locations around the Gulf (see [Figure 1](#)). Synthetic Subsurface Pressure (SSP) were computed by summing the NOS/MEDS sea level (SL) and relevant atmospheric pressure observations as described by [Brown and Irish \(1992\)](#). The suite of coastal SSP records and three bottom pressure (BP) records that characterize the Gulf of Maine pressure (sea level) response and are used to diagnose the accuracy of the model simulations.

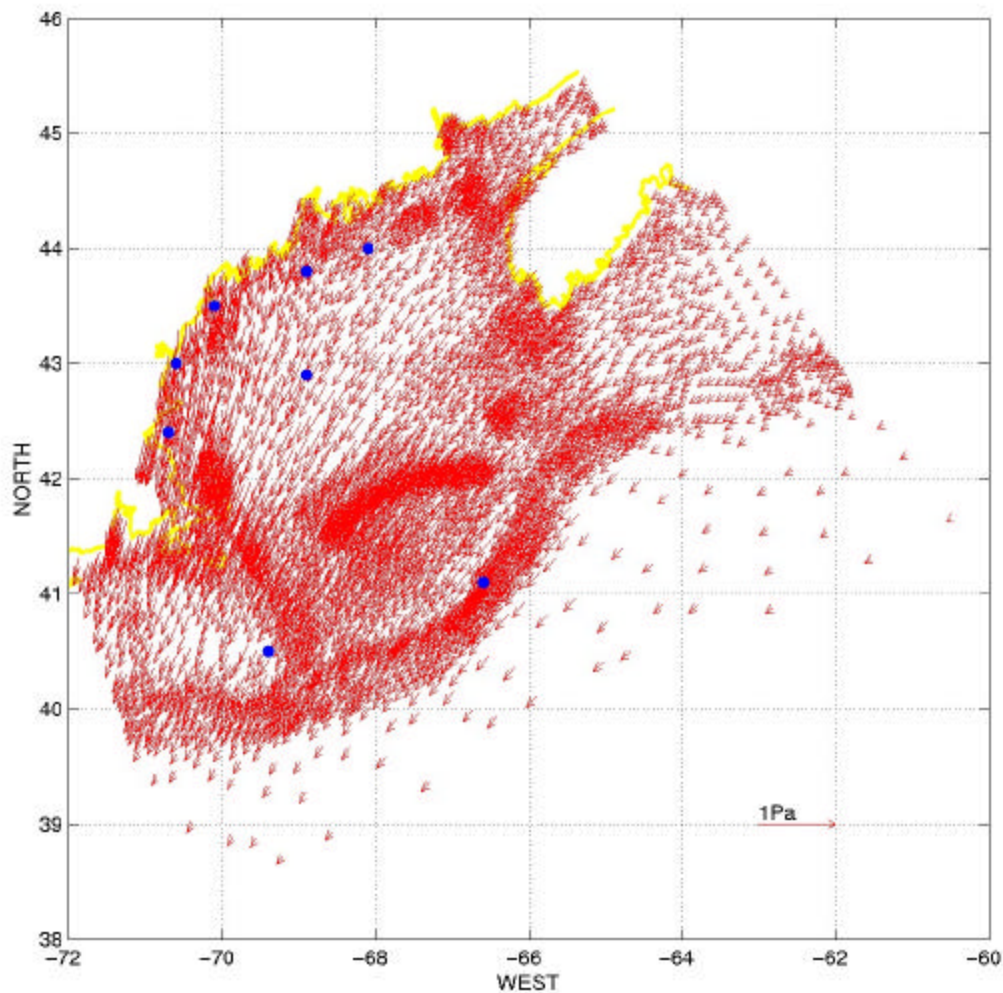


Figure V.2.2 The surface wind stress vectors (scale of 1 Pa or 10 dynes/cm<sup>2</sup>) at each node of the ghsd mesh for 21:00 UTC February 9 1987. These vectors were derived via an optimal interpolation of NDBC wind measurements at indicated sites (dark dot).

**Figure 3 (V.2.2)** The 9 February 1987 2100 UTC example of an optimally-interpolated wind stress field used to drive the QUODDY model runs. The locations of the NDBC/NWS wind measurement stations are indicated.

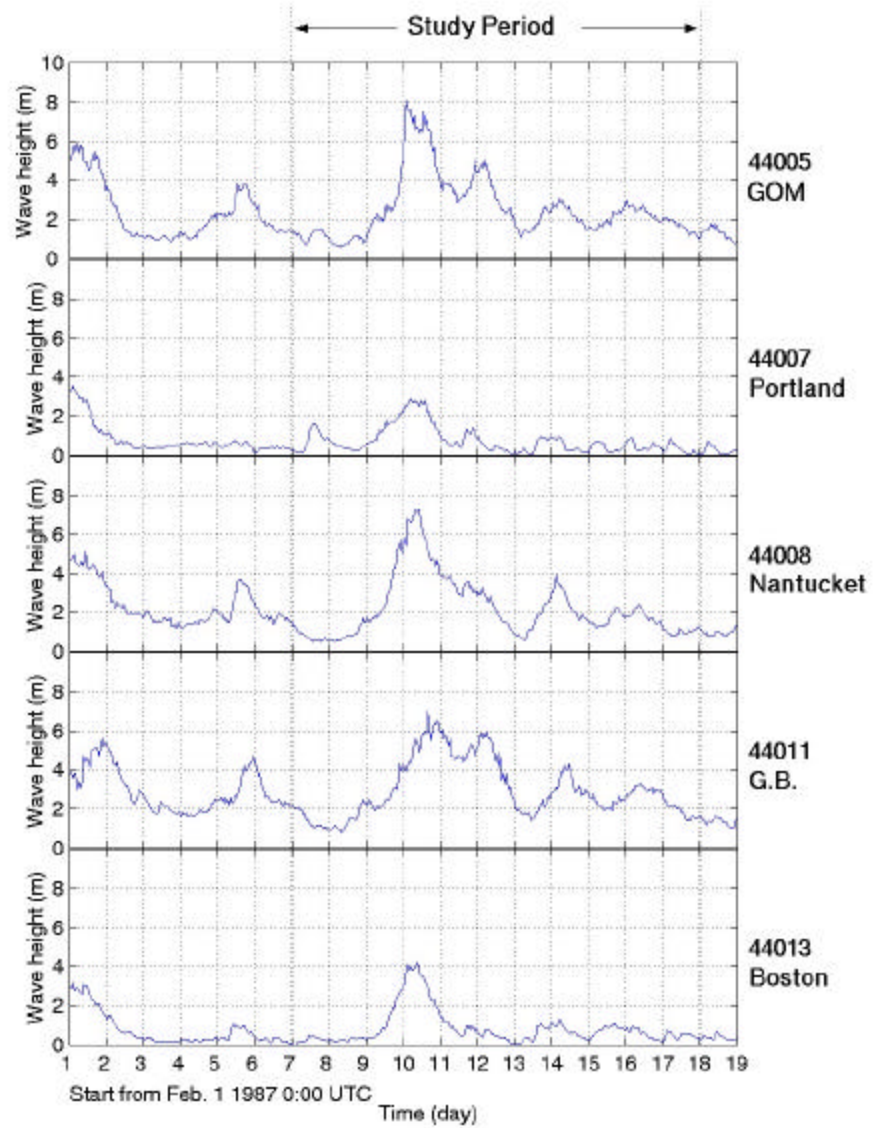


Figure V.2.3 Significant wave height time series at the indicated NDBC stations in the Gulf of Maine. The model study period is indicated on the plot.

Figure 4 (V.2.3) Gulf of Maine NDBC buoy significant wave height hourly time series.

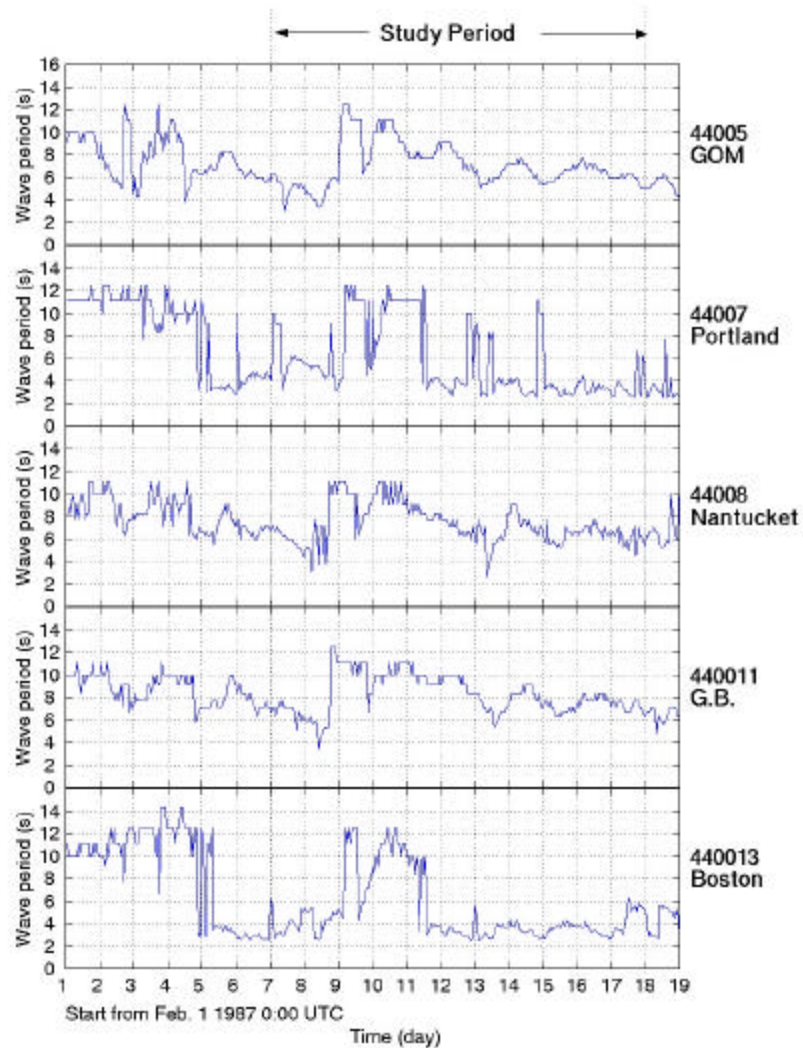


Figure V.2.4 Dominant wave period time series at indicated NDBC stations in the Gulf of Maine. The model study period is indicated on the plot.

**Figure 5 (V.2.4)** Gulf of Maine NDBC buoy dominant wave period hourly time series.

### 3. The Models

#### A. Bottom Boundary Layer Model (BBLM)

The bottom boundary layer model that we used was developed by [Styles \(1998\)](#) under the guidance of S. Glenn. The model consists of three different zones in

which the friction physics differs (Figure 6). Combined wave/current interactions dominate in the lowest (i.e. near-bottom) layer; Current-induced friction dominates in the layer furthest from the bottom. This BBLM model is distinguished from the Grant & Madsen (1979) by having a transition layer between the other two layers.

This BBLM requires inputs of (1) the “slowly” varying current at a near bottom reference depth (in this case from QUODDY) and (2) the instantaneous maximum surface wave-induced bottom water particle excursion and velocity amplitudes. Thus the BBLM outputs a near bottom eddy viscosity and a current profile from which the bottom stress can be estimated. The estimated bottom stress is then converted to an equivalent bottom drag coefficient that can be used in QUODDY.

## B. QUODDY

QUODDY is a nonlinear, hydrodynamic, time-stepping finite element model with advanced turbulence closure (Lynch et al., 1996). The model incorporates the transport of heat, salt, momentum, and two turbulence variables. The QUODDY governing equations are expressed in a Cartesian coordinate system on an f-plane as the following Shallow Water Wave Equation (SWWE)

$$\frac{\eta^2 \mathbf{V}}{\eta t^2} + \tau_0 \frac{\eta \mathbf{V}}{\eta t} + \nabla_{xy} \cdot \left( \tau_0 H \bar{\mathbf{V}} + \mathbf{V}|_{z=\eta} \frac{\eta \mathbf{V}}{\eta t} + \int_{-h}^{\eta} \left[ F_m - \mathbf{V} \cdot \nabla \mathbf{V} + \frac{\mathbf{s}}{\mathbf{r}} (\mathbf{V}_s - \mathbf{V}) \right] dz \right) - g H \nabla_{xy} \cdot \mathbf{V} - f \times (H \bar{\mathbf{V}}) + H \mathbf{y} - C_d |\mathbf{V}_b| \mathbf{V}_b + HR \quad = \frac{\eta Q}{\eta t} + \tau_0 Q \quad (2)$$

where  $\eta$  is the free surface elevation,  $\tau_0$  – a constant,  $H$  – total fluid depth ( $H = h + \eta$ ),  $\mathbf{V} = ui + vj$  -horizontal velocity,  $F_m$  - non-advective horizontal exchange of momentum,  $\mathbf{s}$  – distributed mass source rate,  $g$  – gravity,  $f$  – Coriolis parameter,  $H \mathbf{y}$  - surface boundary forcing, including wind stress and heat/mass transfer, and  $C_d |\mathbf{V}_b| \mathbf{V}_b$  - the quadratic bottom boundary stress. For this application, atmospheric pressure gradient forcing ( $-H \nabla P_{air}/\rho_w$ ) was implemented (following Young et al., 1995) to QUODDY as an added surface forcing agent.

The finite-element method is used to solve (1). The horizontal model domain is discretized by triangular elements with linear basis functions. The vertical is resolved by a terrain-following coordinate system consisting of a string of nodes connected by 1-D linear elements.

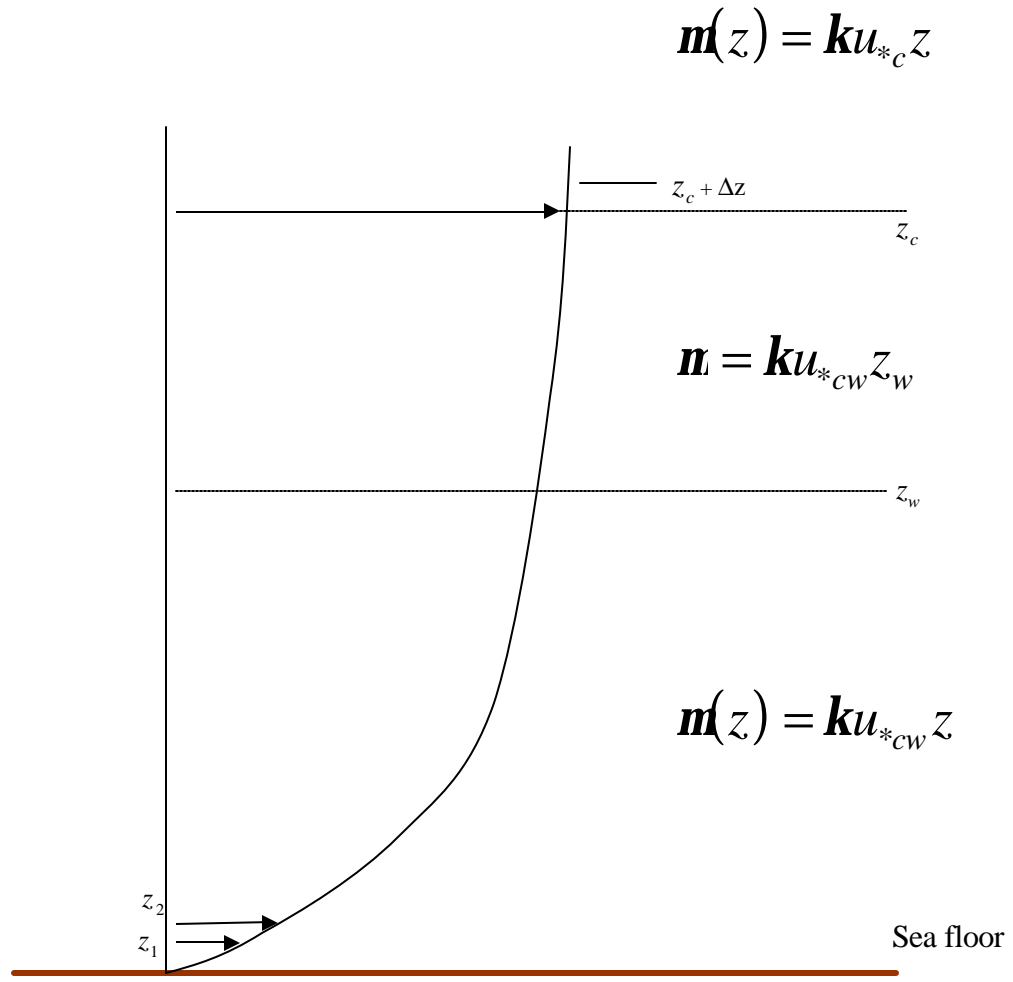


**Figure 6.** Bottom boundary layer model geometry for the [Styles \(1998\)](#) model, which has three boundary layer regions; one for combined wave and current  $0 \leq z \leq z_w$ ; one for the transition layer  $z_w \leq z \leq z_c$ ; and one for current only  $z > z_c$ . The horizontal currents  $u_1$  and  $u_2$  at elevations  $z_1$  and  $z_2$  respectively are used to define the near-bottom stress.

The governing equations are solved subject to conventional boundary conditions at horizontal and vertical boundaries. The boundary conditions on the horizontal surfaces are the (1) specified atmospheric shear stress at the sea surface (see Figure 3 for an example) and quadratic slip at the bottom and (2) kinematic boundary condition on vertical velocity on both surfaces. Lateral boundary conditions on wet boundaries consist of either (1) a specified sea level plus zero

normal flow or (2) a radiation boundary condition. Zero normal velocity is enforced at land "vertical walls" everywhere.

We focus here upon the bottom boundary condition in this study. QUODDY was designed to employ a time-constant bottom drag coefficients ( $C_d$ ) to calculate the quadratic bottom stress. For our reference QUODDY model runs, we used a time and space constant  $C_d$ . However for our other model experiments, we inferred a time-space variable  $C_d$  from the surface wave/current-induced BBLM bottom friction which was consistent with the local QUODDY currents.

The required model forcing was derived from observations. Surface wind stress was computed from National Data Buoy Center (NDBC) wind measurements at the Gulf of Maine NDBC sites shown in Figure 1. The surface wave data needed to force the BBLM were also obtained from NDBC buoys (Figures 4 and 5) as described above.

#### 4. QUODDY Modeling

The GHSD mesh, built by [Holboke \(1999\)](#) (see [Figure 7](#)), was used for these QUODDY calculations. The GHSD mesh resolution varies from about 10km in the Gulf to about 5km near the coastlines. The coastal node of the "upstream" across-shelf open ocean boundary was located at Halifax so that the coastal sea level data available there could be used to specify the time varying sea level boundary condition there.

The model was run in a barotropic mode (i.e. constant density) with steady, homogeneous temperature and salinity fields. The assumed constant temperature of  $T = 6.39^\circ\text{C}$  and assumed constant salinity of  $S = 33.47\text{psu}$  were based on the 15m deep moored temperature and salinity, respectively, in Wilkinson Basin for the February 1987 ([Brown & Irish, 1993](#)). The initial velocity and elevation fields were calculated diagnostically using the model FUNDY5 described in [Lynch et al \(1992\)](#).

A variety of boundary conditions were applied along the different segments of the model boundary. Specifically, inhomogeneous, barotropic radiation boundary conditions ([Holboke, 1999](#)) are imposed on both the "upstream" and the "downstream" across-shelf open ocean boundaries (magenta line; [Figure 7](#)). The  $M_2$  semidiurnal tidal elevation -based on [Lynch et al \(1997\)](#)- and a steady residual elevation - based on [Naimie et al. \(1996\)](#) - are specified along the offshore open boundary (red line; [Figure 7](#)).

Both the semidiurnal  $M_2$  tidal and residual elevation open ocean forcings are imposed along the "upstream" across-shelf boundary (cyan line). One part of the residual elevation forcing was calculated from the initial fields. The other part, called the "smooth-step" extrapolation ([Holboke, 1999](#)) was used to simulate the effect of non-local sea level (i.e. pressure) variability propagating along the

Scotian Shelf into the Gulf of Maine solution. The structure of the "smooth-step" sea level extrapolation is nearly constant across the Scotian Shelf to the shelf break, where it decreases rapidly according to the equation

$$V_{nl} = 1.0 - e^{-(260km-s)/20km}, \quad (3)$$

where s is the distance offshore from Halifax along the boundary. The  $M_2$  tidal forcing and residual elevations calculated from the initial fields are applied to the "downstream" across-shelf boundary.  $M_2$ ,  $M_4$ ,  $M_6$  tidal elevations and zero normal flow are prescribed on the Bay of Fundy boundary.

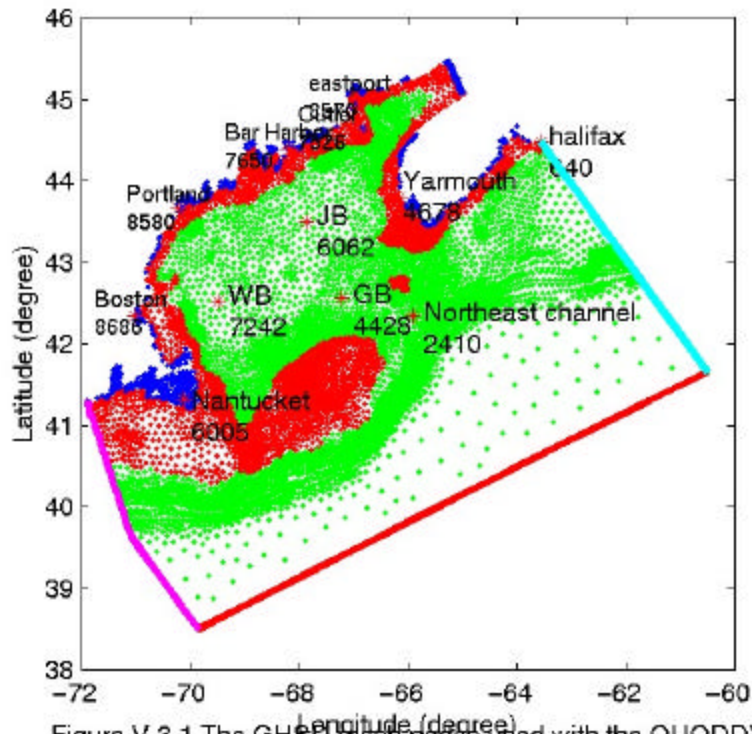


Figure V.3.1 The GHSD mesh nodes used with the QUODDY model. The blue mesh is in depths less than 15m; the red nodes in depths less than 80m and greater than 15m; green nodes are in depths greater than 80m. Red stars locate sea level or bottom pressure observation stations as in Figure I.1.1. The mesh node numbers of these stations are

**Figure 7(V.3.1)** The GHSD mesh for the QUODDY model domain.

The barotropic QUODDY model simulation was run between February 7<sup>th</sup> 0:00 1987 and February 18<sup>th</sup> 21:42 1987 (26  $M_2$  tidal cycles), during which the strong 9-13 February storm occurred. The simulation time step was 21.83203125 sec

(an  $M_2$  tidal period /2048). The first six cycles of the simulation are used to ramp-up the model forcing fields at the open boundaries from zero to full amplitude tides and time/space-varying surface wind stress. During the 2 model-day process, the initial conditions are advection-corrected.

The first set of QUODDY model runs employed constant bottom drag coefficients  $C_d$  values. The second set of QUODDY model runs employed time/space-varying  $C_d$  values that were inferred from with the BBLM. The model results were output 16 times per tidal cycle. The non-tidal model results (averaged over the previous tidal period) were output every quarter of a tidal period.

## 5. QUODDY Model Results: Constant $C_d$

A constant drag coefficient  $C_d = 0.005$  was used for the first QUODDY simulation. These QUODDY sea level results from this run (black lines; [Figure 8](#)) clearly show the tides as well as the response to the 9-10 February storm. To better compare observations and model results, we removed the tides from the model and observed time series. These so-called *subtidal* observed pressure and model sea level time series were formed by first removing the predicted tides and then applying to the detided records a low pass filter, with a cutoff frequency of  $(36)^{-1}$  cph. With the tides removed it is much easier to see that sea level decreases about one day later after the storm began, and remained low for another one and half days after the storm was over.

Subtidal bottom pressure (BP) and coastal synthetic subsurface pressure (SSP) observations are compared to the  $M_2$  tide and wind-forced only model sea elevations in [Figure 9](#). This particular comparison is justified because both SSP and BP observations have been insulated from most of the real atmospheric pressure variability by the approximate inverted barometric response of sea level to atmosphere pressure forcing.

The model sea level results show the same general variability as the observed pressure equivalent sea levels ([Figure 9](#)). In these simulations, more than 60% of the observed sea level variance was captured by the model (Table 1). This QUODDY performance compares with only 31% of the variance captured by a linear harmonic diagnostic model simulation, documented by [Brown \(1998\)](#), and thus represents an improvement.

However, there still are significant differences between these model results and observations in or around the times of the intense storm of February 9<sup>th</sup> to 13<sup>th</sup>. In order to investigate the model sensitivity to different values of the bottom drag coefficient, we conducted two more model runs with  $C_d = 0.0025$  and  $0.0035$  respectively. The standard deviations of observed minus model sea level differences are plotted in [Figure 10a](#) (see [Table 2](#)).

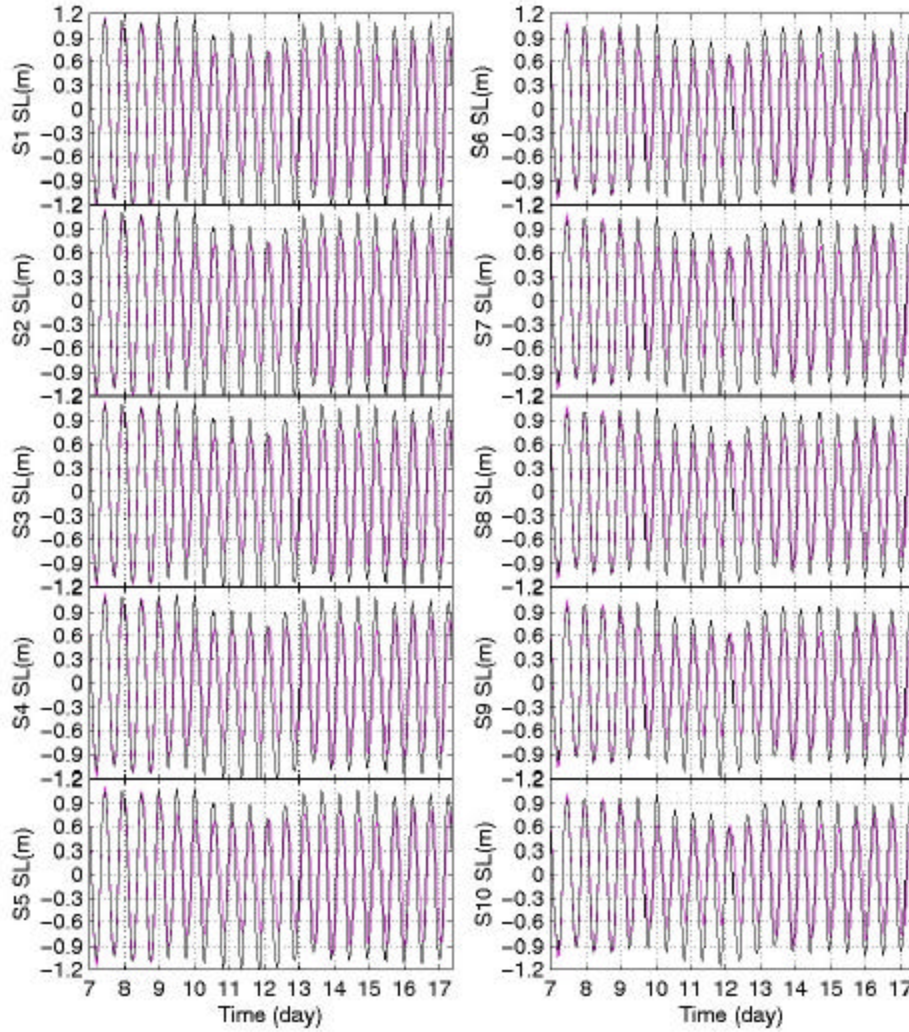


Figure V.4.2 QUODDY model sea level along the transect defined in Figure V.4.1 under constant Cd conditions (black) vs. QUODDY model sea level with space time variable Cd (magenta).

. **Figure 8 (V.4.2)** Tidal time QUODDY (Cd= 0.005) sea level results at the Figure 1 SSP stations

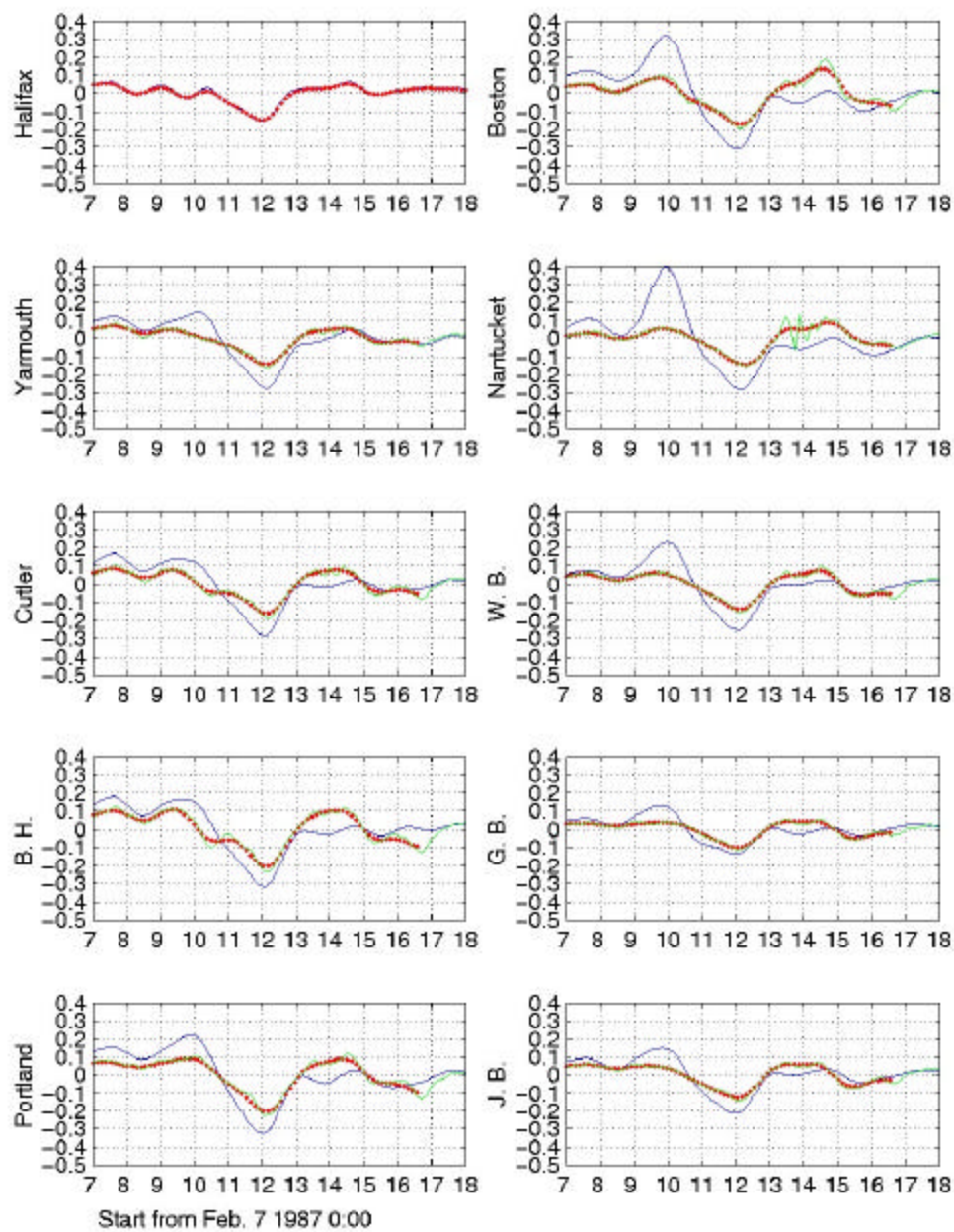
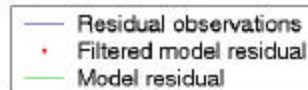


Figure V.4.5. Observed vs. filtered and unfiltered residual model sea level for constant  $C_d = 0.005$ . A lanczos low pass filter with  $0.1733\text{hr}^{-1}$  cut off frequency was used. The abscissa in each panel shows the February 1987 0000 FMT dates.



**Figure 9 (V.4.5)** A comparison of subtidal constant  $C_d$  QUODDY model and observed sea levels at the stations in [Figure 1](#).

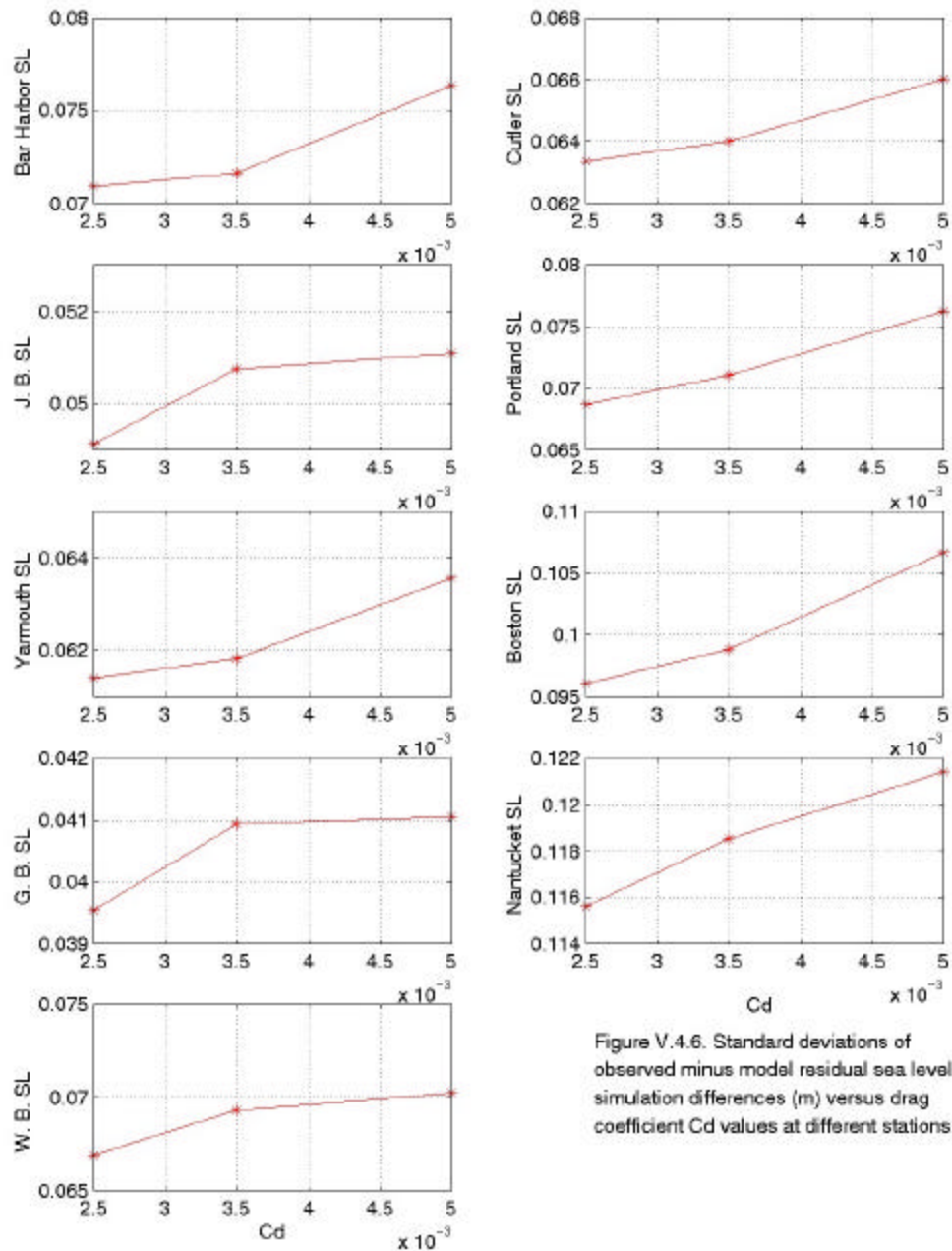


Figure V.4.6. Standard deviations of observed minus model residual sea level simulation differences (m) versus drag coefficient  $C_d$  values at different stations

**Figure 10a (V.4.6)** Standard deviations of subtidal observed minus model sea levels for different constant  $C_d$  values.

The efficiency of the model in simulating reality was assessed by calculating the model skill defined by

$$Model \ Skill = 1 - \left( \frac{1}{N} \sum_{i=1}^N a_i \frac{s_{DPi}^2}{s_{OP}^2} \right) , \quad (4)$$

where, N is the number of time series we have,  $s_{DP}$  is the variance of the sea level difference time series  $s_{OP}$ , which is the variance of the observed sea level time series. We assume the values are equally weighted, i.e.  $a_i = 1$ . These results are plotted in Figure 10b. From these statistics of the observations and model results (Tables 1 and 2), we can see that there are only slight differences between the simulation results for these different Cd values. (Although the model results may be improved by using very small drag coefficient Cd, thus is not realistic during a stormy period). Thus we do not expect an improvement of simulation results by just changing Cd values over this range.

97

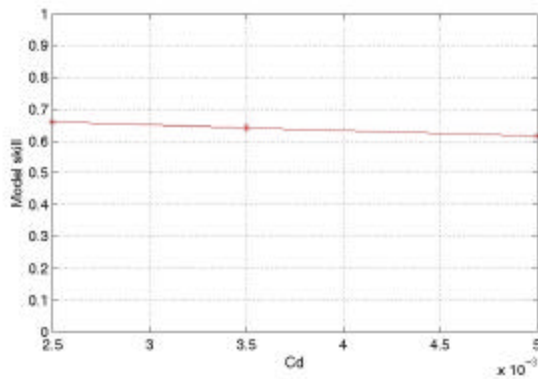


Figure V.4.7. Model Skill versus Drag coefficient Cd

**Figure 10b (V.4.7).** Skill level of QUODDY model sea levels for different constant Cd values.

**Table 1.** Comparison of standard deviations of observed and model sea level variability for period between 7 and 17 February. Model results for cases with different drag coefficients; Cd = 0.0025, 0.0035, and 0.0050 respectively

	Observations	Cd = 0.0050	Cd = 0.0035	Cd =0.0025
Bar Harbor	0.1318	0.0904	0.0843	0.0844
Cutler	0.1168	0.0699	0.0656	0.0656
Portland	0.1410	0.0845	0.0779	0.0786
Yarmouth	0.1095	0.0572	0.0569	0.0575
Boston	0.1518	0.0785	0.0641	0.0644
Nantucket	0.1550	0.0594	0.0501	0.0541
G. B.	0.0665	0.0429	0.0391	0.0401
J. B.	0.0924	0.0573	0.0510	0.0522
W. B.	0.1137	0.0614	0.0553	0.0581
Average	0.1198	0.0668	0.0605	0.0617

**Table 2.** Comparison of the standard deviations of the variability of observed minus model sea level differences for period between 7 and 17 February. Model results for cases with different drag coefficients - Cd = 0.0025, 0.0035, and 0.0050 respectively

	Observations	Difference Cd = 0.0050	Difference Cd = 0.0035	Difference Cd =0.0025
Bar Harbor	0.1318	0.0764	0.0716	0.0709
Cutler	0.1168	0.066	0.064	0.0634
Portland	0.141	0.0762	0.0711	0.0687
Yarmouth	0.1095	0.0636	0.0618	0.0614
Boston	0.1518	0.1067	0.0989	0.0961
Nantucket	0.155	0.1214	0.1185	0.1156
G. B.	0.0665	0.041	0.0409	0.0395
J. B.	0.0924	0.0511	0.0507	0.0491
W. B.	0.1137	0.0702	0.0693	0.0669
Average	0.1198	0.0747	0.0719	0.0702

We also present the simulation results from a transect of stations between Portland and Wilkinson Basin ([Figure 11](#)). These QUODDY sea level results (black lines; [Figure 9](#)) clearly show the as well as the response to the 910 February storm. Detailed model current results have been extracted from the model transect too, and two representative examples of station S1 and S2 are presented in [Figure 12 and 13](#). In contrast with the sea level response, the currents are very much enhanced during the storm period.

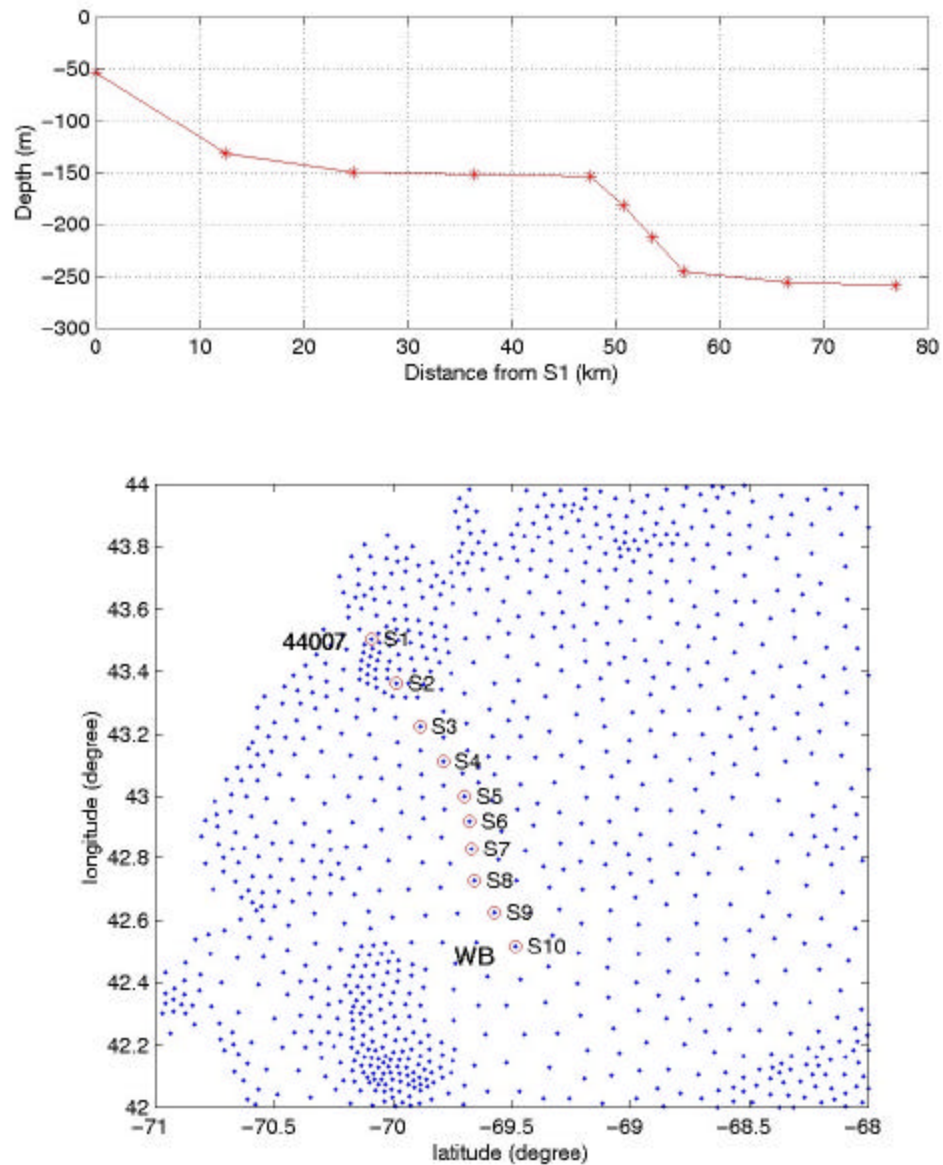


Figure V.4.1. The upper panel shows the cross section of the transect defined between Portland (44007) and Wilkinson Bason (WB), the lower panel shows the location of these stations (circles).

**Figure 11 (V.4.1)** A map of QUODDY model result sampling stations along a transect between Portland and center Wilkinson Basin (below); depths (above).

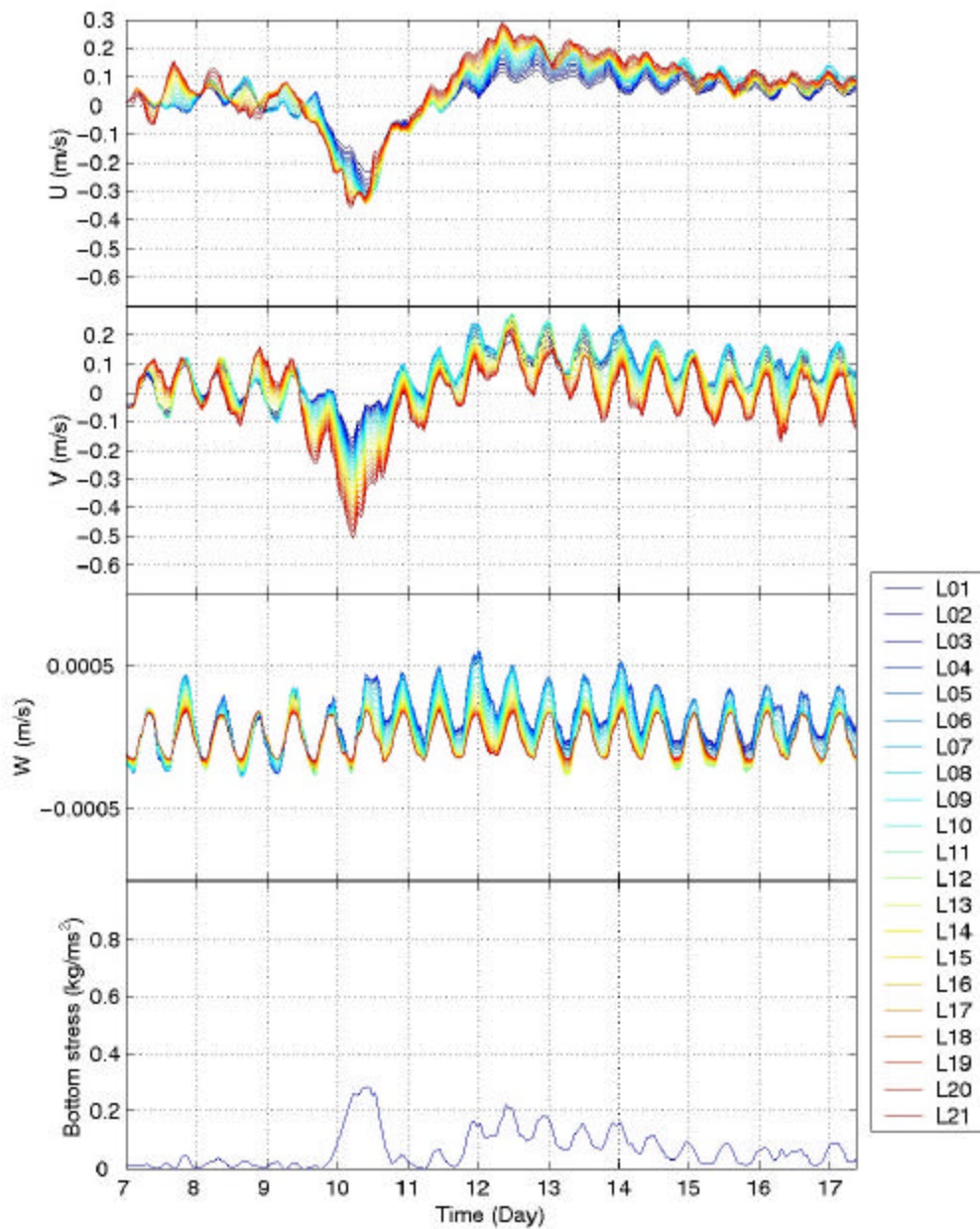


Figure V.4.3. Current time series at every layer from bottom to surface at stations S1  
in the legend L01 is the bottom layer, and L21 is the surface layer

**Figure 12(V.4.3)** Tidal time QUODDY ( $C_d = 0.005$ ) series from station S1. In order from the top panel; (a) eastward current at 21 levels; (b) northward current at 21 levels; (c) upward current at 21 levels; (d) bottom stress;

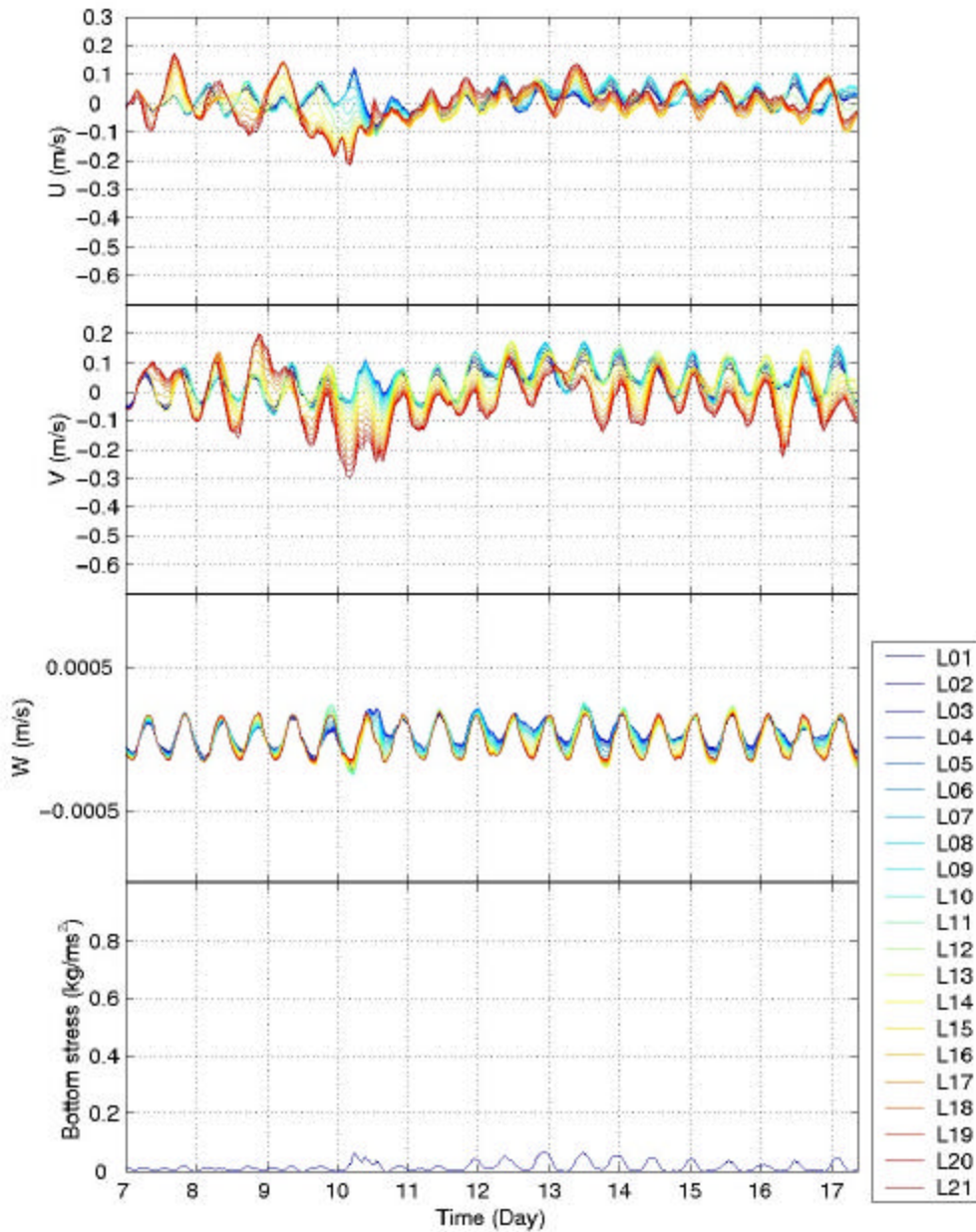


Figure V.4.4. Current time series at every layer from bottom to surface at stations S2 in the legend L01 is the bottom layer, and L21 is the surface layer

**Figure 13 (V.4.4).** Tidal time QUODDY ( $C_d = 0.005$ ) series from station S2. In order from the top panel; (a) eastward current at 21 levels; (b) northward current at 21 levels; (c) upward current at 21 levels; (d) bottom stress;

For the first QUODDY simulation, we used a constant drag coefficient  $C_d = 0.005$ . We present the simulation results from a transect of stations between Portland and Wilkinson Basin (Figure 8). These QUODDY sea level results (black lines; Figure 9) clearly show the tidal variability as well as the response to the 9-10 February storm. Sea level decreases about one day after the storm onset and remained low for another one and half days after the storm was over. Detailed model current results have been extracted from the model transect too, and two representative examples of station S1 and S2 are presented in Figures 12 and 13. In contrast with the sea level response, the currents are very much enhanced during the storm period.

Hodographs of the subtidal model velocity profiles for these stations are presented for two distinct times on Feb. 10 1987. At 5:37:32 UTC (Figure 14) shows that current vectors at most of the stations are generally  $45^\circ$  to the right of the wind stress at the surface, and below that smoothly rotate to the right down to a depth of about 100m deep. The velocity structure is very Ekman-like, with surface speeds ranging from 0.31m/s (station 10) to 0.56m/s (station1) or about 2% of the wind speed ( $\sim 20$ m/s) at the time. At 22:42:11 UTC (Figure 15), the wind speed was much smaller ( $\sim 11$ m/s) with correspondingly smaller current speeds. Even so, the Ekman spiral still penetrated to depths of about 100m – consistent with our expectation. This suggests that the wind speed doesn't influence how deep the Ekman rotation can penetrate. The surface current direction relative to the wind direction ranged from  $20^\circ$  to  $67^\circ$  to the right of the wind stress. This is significantly different than the earlier observations, which were influenced by much stronger winds.

## **6. QUODDY Model Results: Time/Space-Dependent Bottom Drag Coefficient**

In order to simulate the Gulf of Maine response with time/space-variable bottom drag coefficients, we conducted a suite of coupled wind-forced QUODDY/BBLM model simulations with the same wind forcing as in the constant  $C_d$  cases. However in this case, waves were needed to force the BBLM. As shown in Figures 4 and 5, there were significant differences in the wave height and dominant wave period at the different NDBC stations. So we divided that part of the Gulf with depths  $< 80$ m into 5 sub regions and used the wave information from the relevant NDBC buoys (Figure 16). The hourly NDBC significant wave height and dominant wave period data were interpolated to the QUODDY model time interval (21.83203125 sec). These data were converted using linear wave theory to the maximum bottom wave velocity and maximum bottom excursion amplitude required by the BBLM.

The model sea levels at stations along the transect are compared with the constant  $C_d$  QUODDY-derived sea level in Figure 8. We see that the space-time variable  $C_d$  model sea level response is (1) more damped than that in the

constant Cd case and (2) responds to the storm much more rapidly than the other case and is depressed more than 5 days after the storm ends. The comparison of model and observed subtidal sea levels (Figure 17) and the standard deviations (Table 3) show that the model with space-time variable bottom stress produces less Gulf-wide sea level variance than the constant Cd calculations (see Table 1).

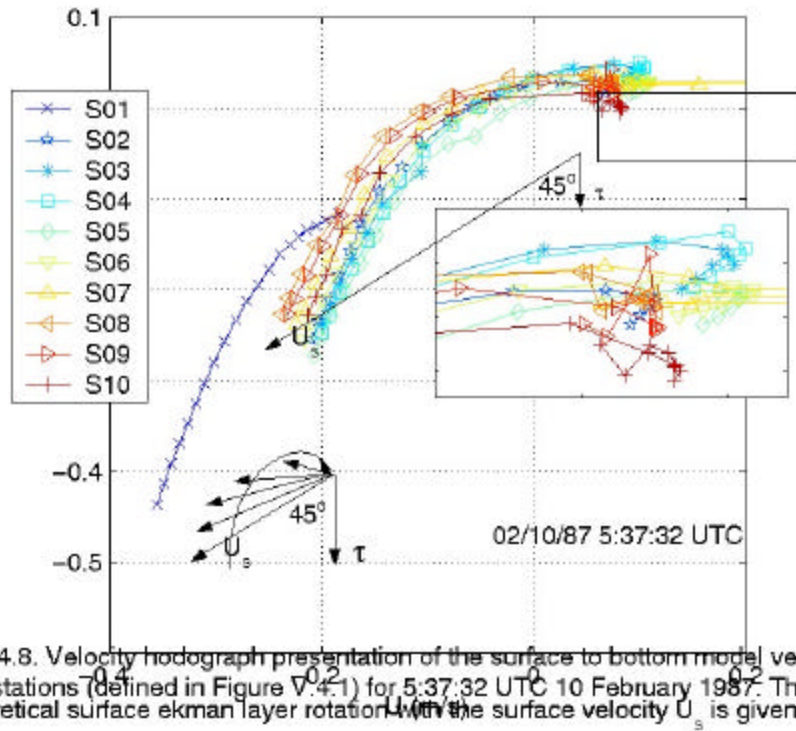


**Figure 14(V.4.8)** Subtidal model current hodographs at the different transect stations for 0537 UTC 10 February 1987.

A possible reason for this difference is that the wave information in the Gulf is inadequate for our purposes. For example, Figure 17 suggests the wave-induced bottom stress decreases the sea level response (February 10<sup>th</sup>), or it can also enhance the sea level response (February 13<sup>th</sup>). We expect that a much more detailed understanding of the Gulf of Maine wave structure during the model simulation period may result in a better model behavior. Another possible reason for the problem was our neglect of atmospheric pressure forcing.

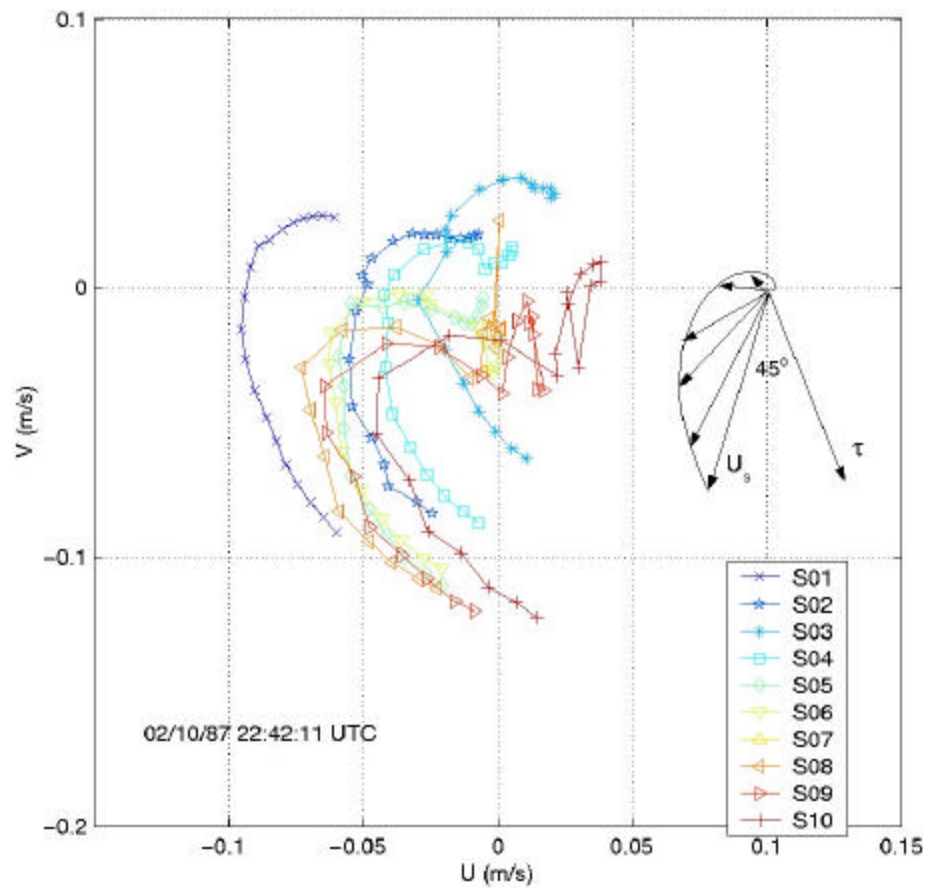


Figure V.4.9. Velocity hodograph presentations of the surface to bottom model velocity for the transect stations (defined in Figure V.4.1) for 22:42:11 UTC 10 February 1987. The wind stress and theoretical surface Ekman layer rotation with the surface velocity  $U_s$  is given for reference.

**Figure 15 (V.4.9)** Subtidal current hodographs at the different transect stations for 2242 UTC 10 February 1987.

The cross correlation analysis of the atmosphere pressure and residual sea level at Portland and Boston for the winter 1987 (1 Dec. 1986 to Feb. 30, 1987) (Figure 18) shows that only 25% of the sea level variability is correlated with atmospheric pressure at the coast. And the atmospheric pressure / sea level

transfer coefficient  $T_{ap-sl}$  (which is defined according to:  $T_{ap-sl} = \frac{R_{ap-sl}}{R_{ap-ap}}$ , where

$R_{ap-sl}$  is the cross covariance of atmosphere pressure and sea level and  $R_{ap-ap}$  is the auto covariance of atmosphere pressure) calculated for these two stations (Table 4) also shows that 18% (6%) of the atmosphere pressure at Portland (Boston) penetrates to the bottom. These two calculations mean that the inverted barometric sea level response is very imperfect. Thus the coastal Gulf is not insulated from atmospheric forcing, but the neglect of atmospheric pressure in the model forcing is not the major problem here.

Still another reason for the difference may be that we underestimate the wind stress. Our estimated wind stress in the whole Gulf using wind observations at only seven stations is not likely to resolve local winds very well. Also, in our model calculation, we use the Large and Pond (1981) formulae to calculate wind stress, a standard air density value  $1.22\text{kgm}^{-3}$  are used for air density all the time. During our calculation period, the winds came from north, it brought dry cold air to the Gulf, so there is a possibility that we underestimated air density, hence underestimated the wind stress. After increasing the wind stress by 60%, one more model run was conducted using constant  $Cd = 0.005$ . The comparison of model and observed residual sea levels are shown in Figure 19 and a clear comparison of these three different calculations (a).  $Cd = 0.005$  with Large and Pond (1981) wind stress, (b) BBLM derived  $Cd$  with Large and Pond (1981) wind stress and (c)  $Cd = 0.005$  with increased wind stress, at Portland are shown in Figure 20. We can clearly see from Figures 19 and 20 that the model results are very much improved with the increased wind stress. More work will be done to research on this later.

**Table 4.** The atmospheric pressure / sea level transfer coefficient  $T_{ap-sl}$ , at Portland and Boston.

Station	$R_{ap-sl}$	$R_{ap-ap}$	$T_{ap-sl}$
Portland	-0.0098	0.0119	-0.8235
Boston	-0.0109	0.0115	-0.9478

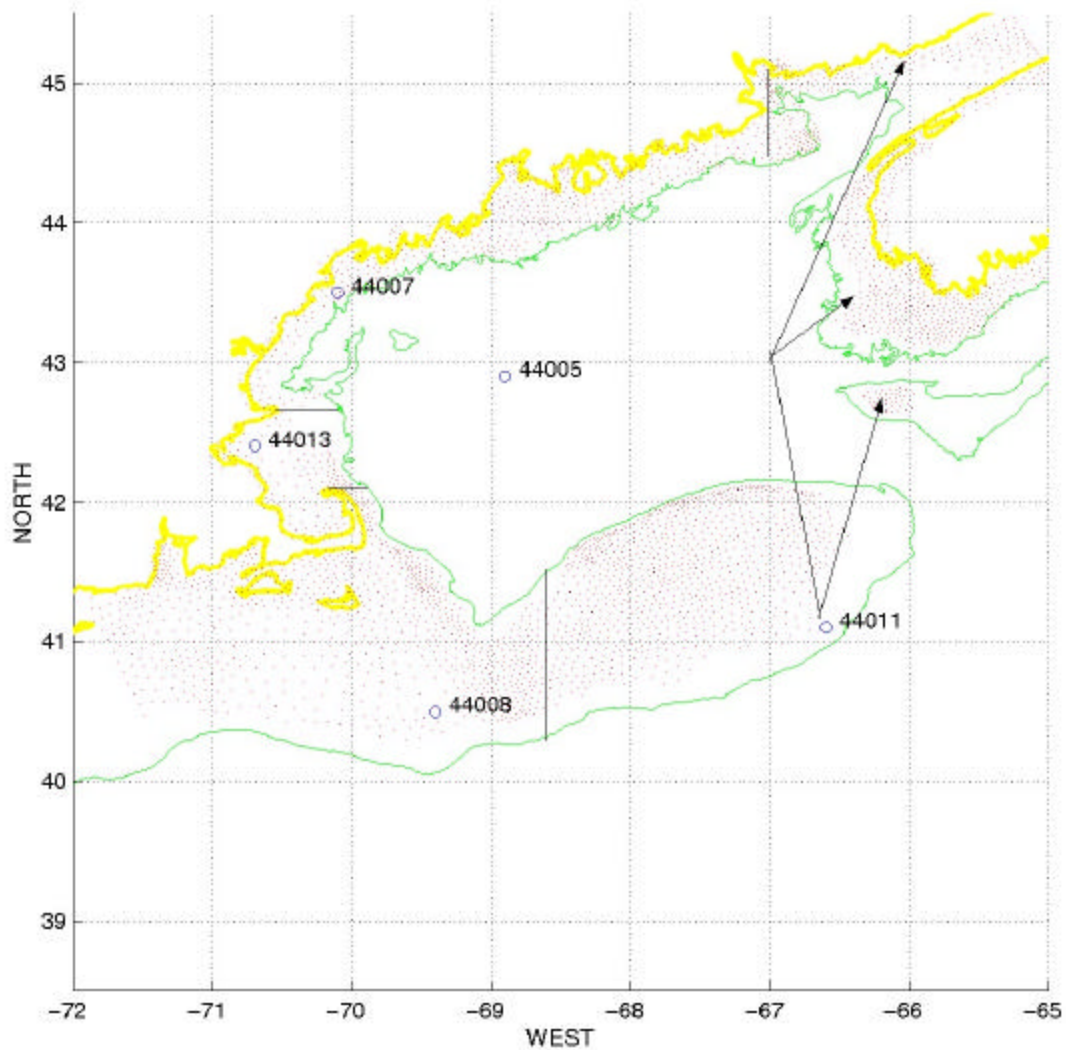


Figure V.2.5 Map of the Gulf of Maine, showing the wave stations (o) in the Gulf and the separated regions with depth less than 80m for different wave stations. The line in the Gulf shows 100m isobath.

**Figure 16 (V.2.5).** A map of the Gulf of Maine showing which wave measurements were used with the BBLM in particular coastal regions.

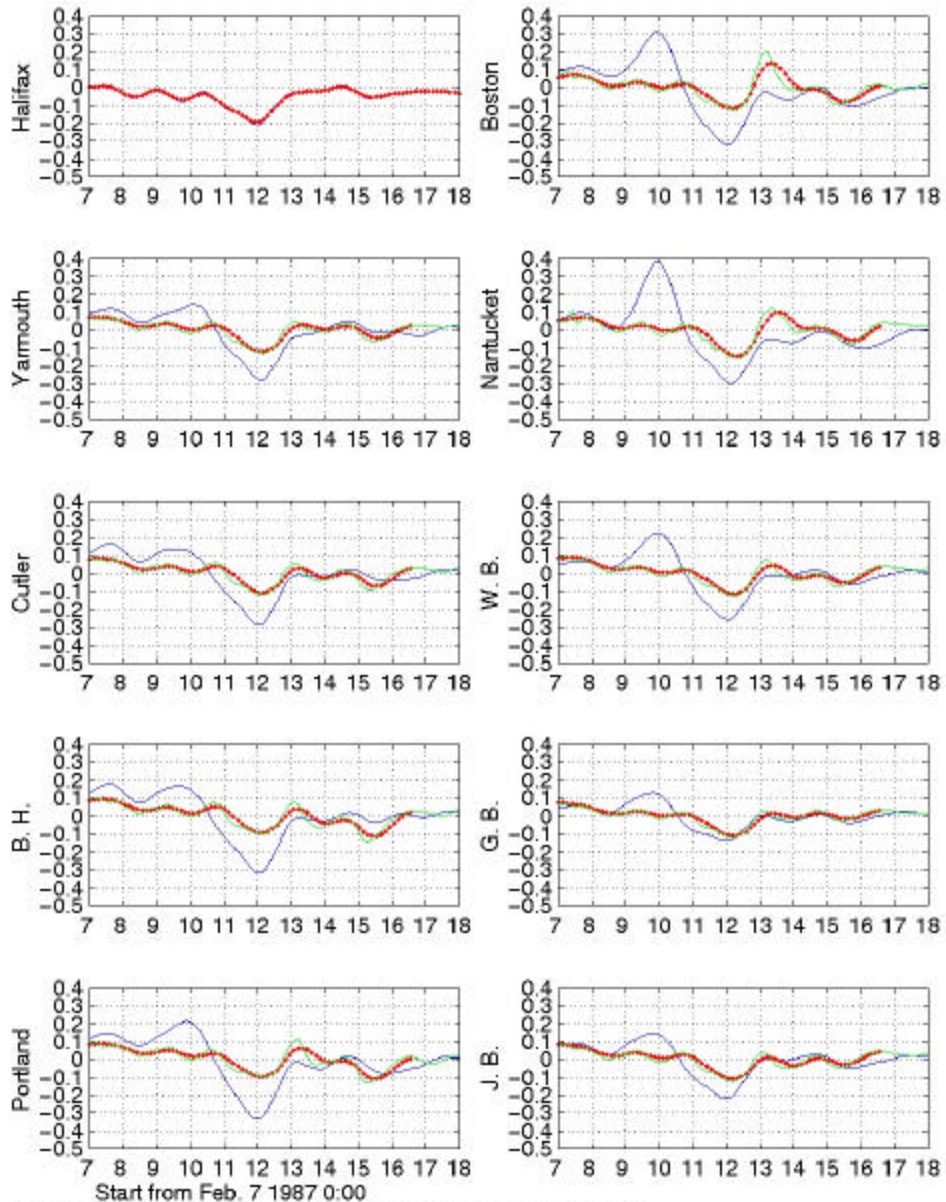


Figure V.5.1. Observed vs. filtered and unfiltered residual model sea level for time-space variable Cd. Use BBLM to calculate Cd. The low passed filtered model calculation results used a lanczos low pass filter with  $0.1733\text{hr}^{-1}$  cut off frequency. The abscissa for each panel indicates midnight at the beginning of the February date indicated.

**Figure 17(V.5.1)** Comparison of subtidal space-time variable Cd QUODDY model 9 without atmospheric pressure forcing) and observed sea levels at the stations in Figure 1.

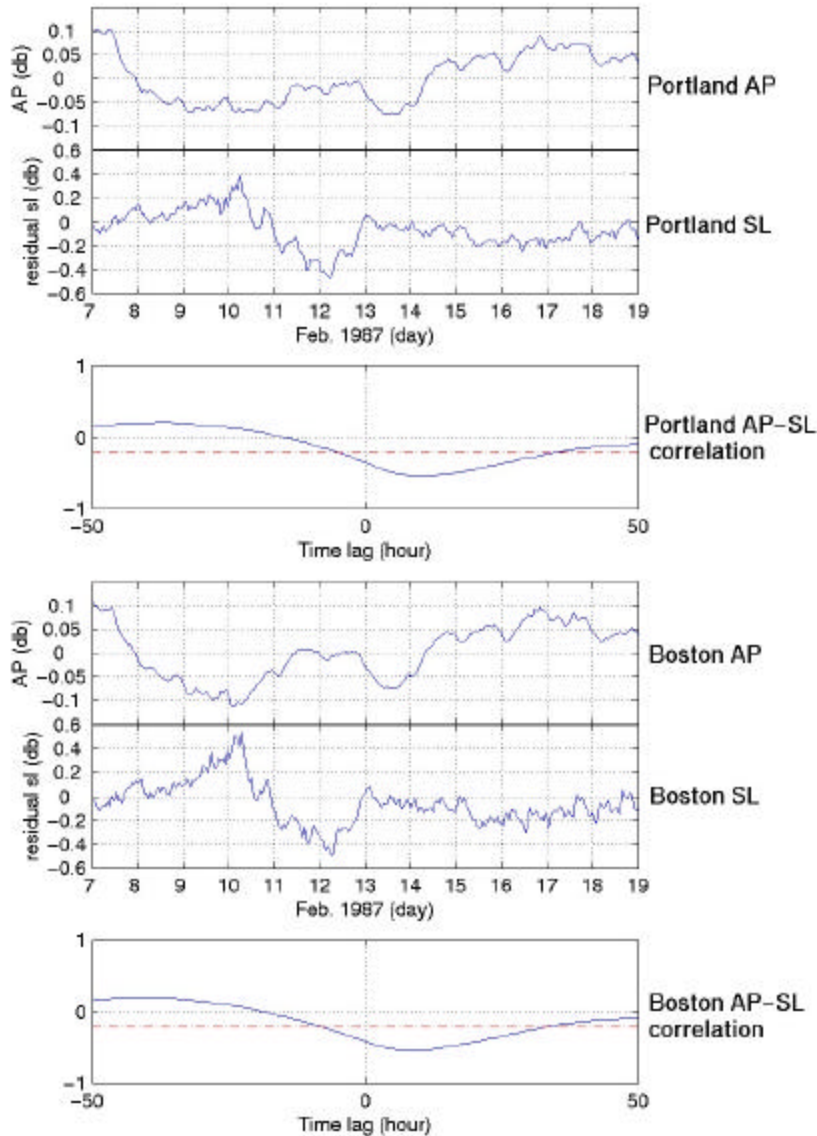


Figure V.5.2 Portland and Boston atmospheric pressure (upper), residual sea level (middle) for Feb. 7 ~ 18 1987. The bottom panel shows correlation between air pressure and residual sea level for winter 1987.

**Figure 18(V.5.2)** Comparison of inverted barometric response at Portland and Boston.

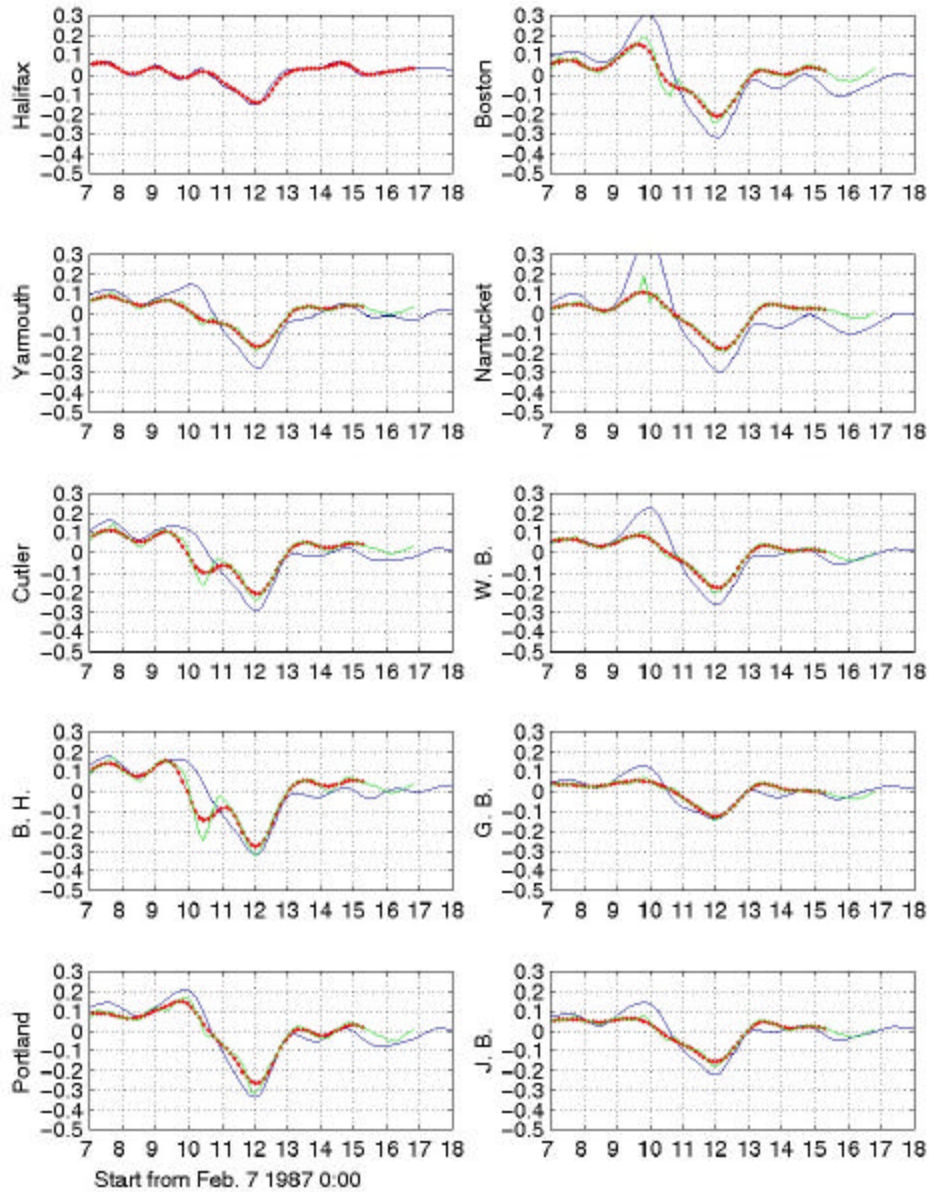


Figure V.5.3. Observed vs. filtered and unfiltered residual sea level for model run for "enhanced" wind stress. The low pass filtered calculation results for  $C_d = 0.005$  used a lanczos low pass filter with  $0.1733\text{hr}^{-1}$  cut off frequency. The x coordinate for each panel showing days.

—	Observations
—+	Filtered Calculations
—	Calculations

**Figure 19 (V.5.3)** Comparison of subtidal observed and model sea levels. In this case, the QUODDY model was run with constant  $C_d$  and "enhanced" wind stresses (but without atmospheric pressure forcing).

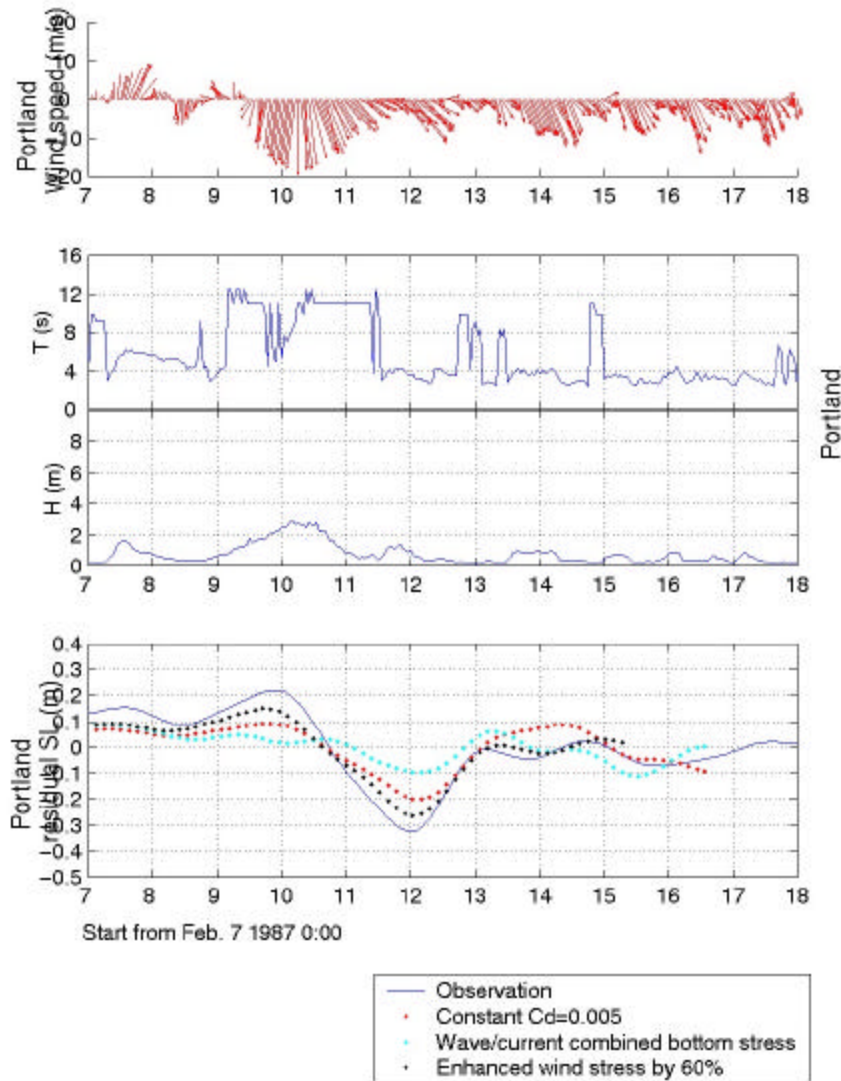


Figure V.5.4. (Upper) Wind speed at Portland; (Middle) Wave information at Portland T: dominant wave period, H: significant wave height, (Bottom) Comparison of QUODDY model residual sea level for three different simulations vs. Observations at Portland

**Figure 20 (V.5.4)** Composite comparison of observed and modeled sea levels at Portland.

## 7. QUODDY Model Section Conclusion

A strong Ekman rotation (see [Figures 14 and 15](#)) was shown in the current results from the [Figure 11](#) stations along the transect. The detided surface current appears to be 3% of the wind speed. The Ekman rotation in the model currents penetrates to a depth of about 100m - independent of the wind speed. The surface current direction seems to be related to the wind speed. For example, for a wind speed of 20m/s, the surface current direction is nearly 45° to the right of the wind direction, while for wind speeds less than 11m/s, the surface current direction varies from 20° to 67° to the right of the wind direction.

The comparison of model residual sea levels with observations shows that the model calculation with constant  $C_d$  can capture more than 60% of the observed variance, compares with only 31% of the variance captured by the linear harmonic model results of [Brown \(1998\)](#). This represents a significant improvement in the modeling. However, there still are large differences between model results and observations in or around the times of the intense storm, especially within the period of the storm (February 9<sup>th</sup> to 13<sup>th</sup>).

In order to improve the calculation results, the time and space variable  $C_d$  supplied by the BLM model was tested. For a number of possible reasons, we saw no improvement to the model results. Upon inspection we found that the model ocean storm response depends more on wind stress than bottom stress. We expect that these improvements in our understanding of the storm-forced response of the Gulf of Maine will come with a more detailed understanding of the waves in the whole Gulf of Maine, a better understanding of the wind stress calculation in the Gulf, and the including of atmosphere pressure into the model forcing.

## 8. Acknowledgements

This research benefited greatly from our affiliation with Daniel Lynch's Numerical Methods Laboratory in the Thayer School at Dartmouth College. The New Hampshire/Maine Sea Grant Program provided salary support through grant R/CE-122. The NOAA/UNH Cooperative Institute for Coastal and Estuarine Environmental Technology, NOAA grants NA77OR0357, NA87OR0512, NA87OR338 purchased the SGI Inc Origin 200 computer that made this work possible

## 9. References:

- Brown, W.S., 1998. Wind-forced pressure response of the Gulf of Maine, *Journal of Geophysical Research*, 103 (C13), 30, 661-30,678.
- Brown, W.S. and J.D. Irish, 1992. The annual evolution of geostrophic flow in the Gulf of Maine, *Journal of Physical Oceanography*, Vol. 22, No. 5, 445-473.
- Brown, W.S. and J.D. Irish, 1993. The annual variation of water mass structure in the Gulf of Maine, *Journal of Marine Research*, 51, 53-107.
- Holboke, Monica J., 1999. Variability of the Maine Coastal Current under Spring Conditions. Phd. Dissertation, Thayer School of Engineering Dartmouth College.
- Large, W. G. and S. Pond, 1981. Open Ocean Momentum Flux Measurements in Moderately Strong Winds. *Journal of Physical Oceanography*, 11, 639-657.
- Lynch, D. R., F. E. Werner, D. A. Greenberg, and J. W. Loder, 1992. Diagnostic model for baroclinic, wind-driven and tidal circulation in shallow seas. *Continental Shelf Research*, Vol. 12, 37-64.
- Lynch, D. R., J. T. C. Ip, C. E. Naimie, and F. E. Werner, 1996. Comprehensive coastal circulation model with application to the Gulf of Maine, *Continental Shelf Research*, 16, 875-906.
- Lynch, D. R., M. J. Holboke, and C. E. Naimie, 1997. The Maine Coastal Current: Spring Climatological Circulation. *Continental Shelf Research*, Vol. 17, 605-634.
- Naimie, C. E., J. W. Loder, and D. R. Lynch, 1996. Seasonal variation of the three-dimensional residual circulation on Georges Bank. *Journal of Geophysical Research*, Vol. 101, 6469-6486,
- Styles, B.R, 1998. A continental shelf bottom boundary layer model: development, calibration and applications to sediment transport in the Middle Atlantic Bight. Phd. Dissertation, Institute of Marine Studies, Rutgers University.
- Young B., Y. Lu, and R. Greatbatch, 1995. Synoptic bottom pressure variability on the Labrador and Newfoundland continental shelves. *Journal of Geophysical Research*, 100, C5, 8639- 8653.